

# A methylenic group binds guanidinoacetic acid to glycine and serine in two novel copper(II) complexes: Synthesis, X-ray structure and spectroscopic characterization

O. Versiane <sup>a</sup>, B.L. Rodrigues <sup>b</sup>, J.L. de Miranda <sup>c</sup>, Joanna Maria Ramos <sup>a</sup>,  
Claudio A. Téllez S <sup>d</sup>, J. Felcman <sup>a,\*</sup>

<sup>a</sup> Departamento de Química, Pontifícia Universidade Católica do Rio de Janeiro, Rua Marquês de São Vicente 255, Gávea, 22451-900 Rio de Janeiro, RJ, Brazil

<sup>b</sup> Instituto de Física de São Carlos, Universidade de São Paulo, São Carlos, SP, Brazil

<sup>c</sup> Instituto de Química, Departamento de Química Inorgânica, Universidade Federal do Rio de Janeiro, RJ, Brazil

<sup>d</sup> Instituto de Química, Universidade Federal Fluminense, Niterói, RJ, Brazil

Received 7 February 2007; accepted 18 May 2007

Available online 2 June 2007

## Abstract

New condensed amino acids were observed in two Cu(II) complexes, both involving guanidinoacetic acid (GAA). The copper(II) complexes, **1** and **2**, were synthesized and characterized by X-ray crystallography and infrared spectroscopy. Vibrational assignments were performed with the aid of density functional theory (DFT) calculations. Both complexes present an elongation of the carbon chain of the starting amino acid, GAA. One methylenic group binds GAA to the other amino acid, which can be glycine or serine. Complex **1** presents a new condensed synthetic amino acid, glycine-3-*N*-methylguanidino acetic acid (Gly-mGAA) that is the result/product of the reaction between GAA and glycine, with an addition of one carbon in the chain. In complex **2**, a similar ligand to Gly-mGAA was observed, but in this case it is a product of the reaction between GAA and serine, that is, serine-3-*N*-methylguanidino acetic acid (Ser-mGAA). Gly-mGAA and Ser-mGAA coordinate to Cu(II) through two nitrogen atoms and two oxygen atoms. In addition, we attempt to propose the mechanism for formation of Ser-mGAA and Gly-mGAA in two steps. The first one involves a deamidation reaction between two GAA species, producing the intermediate *N,N'*-guanidinodiacetic acid. The second step involves a decarboxylation process between GAA and Ser or Gly.

© 2007 Elsevier Ltd. All rights reserved.

**Keywords:** Guanidinoacetic acid; Copper(II); Methylation; Glycine; Serine

## 1. Introduction

Guanidinoacetic acid (GAA) (Fig. 1) has recently drawn special attention due to the discovery of a disorder in the guanidinomethyltransferase (GAMT) enzyme known as GAMT deficiency which is a recessively inherited autosomal disorder of creatine biosynthesis. GAA is an essential

precursor of creatine, which in turn is indispensable to the energy metabolism in muscles. It is synthesized mainly in the kidneys from arginine and glycine by glycine-aminotransferase [1–5].

GAMT catalyzes the transfer of the methyl group from *S*-adenosyl-methionine (*S*-AdoMet) to GAA, which is the final step of creatine biosynthesis. Its deficiency is characterized by creatine depletion and tissue accumulation of GAA. Symptoms of this disorder include development delay or regression, mental retardation, severe abnormalities in cognitive speech, muscular hypotonia, involuntary

\* Corresponding author. Tel.: +55 21 31141329; fax: +55 21 31141637.  
E-mail address: [felcman@rdc.puc-rio.br](mailto:felcman@rdc.puc-rio.br) (J. Felcman).

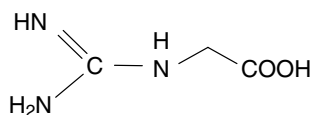


Fig. 1. Structure of guanidinoacetic acid.

extrapyramidal movements, epilepsy, as well as autistic or self-aggressive behavior in older patients [6–11].

Besides being involved in GAMT deficiency, GAA participates in a number of other biological processes. First, since it is synthesized prior to creatine and in the renal tubules, its urinary excretion rate may be used as a sensitive indicator of early-stage nephropathy [12–14]. GAA can also act as a neurotoxin and neuromodulator since it is a partial agonist of the GABA-A receptor and inhibitor of  $\text{Na}^+/\text{K}^+$ -ATPase activity [15,16]. Other GAA biological roles are related to cholesterol production [17], thyroid dysfunction [18], epileptic seizures [19], hepatic encephalopathy [20] and insulin regulation [21]. It is also well known that levels of GAA are increased in the cerebral cortex after hyperbaric oxygenation, probably due to a decrease in arginase activity, which causes an increase of both Mn and Cu, Zn-superoxide dismutase [18]. In addition, a significant decrease in the urinary excretion of GAA has been observed after cisplatin treatment in patients with urinary tract neoplasm [22].

This diversity in participation of GAA in several subject areas should be related to the pool of possible chemical reactions that it can present. We have already studied some of GAA properties by analyzing its coordination to some metal ions of biological interest. GAA complexes with Mn(II), Co(II), Ni(II), Cu(II), Zn(II), Cd(II) and Pb(II) were studied potentiometrically in aqueous solution where besides determining the stability constants of the principal species, an  $\alpha$ -nitrogen and oxygen-carboxylate coordination to the metals was proposed [23]. From synthesized GAA powder complexes with Cr(III), Co(II), Ni(II), Cu(II) and Zn(II), the same kind of coordination, that is, through  $\alpha$ -nitrogen and oxygen-carboxylate, was observed by infrared, ultraviolet–visible spectroscopies and electron paramagnetic resonance [24]. The involvement of  $\alpha$ -nitrogen from GAA in the metal coordination is in agreement with the biological step of its methylation that occurs at the same site/atom.

We have also studied the guanidino-carboxylate interactions between GAA and glutamic acid or aspartic acid in the presence of Cu(II) in aqueous solution [25]. These interactions are biologically very important since they are observed in the substrate fixation of Cu, Zn-superoxide dismutase and of carboxypeptidase A besides being identified in the complex formed by a human immunodeficiency virus and the receptor on the cell wall [26,27]. From our studies we could observe that the values of stability constants of the ternary complexes involving both GAA and Glu or Asp (Cu(II):GAA:L systems, L = Glu or Asp) were higher

than the expected due to the possibility of occurrence of these interactions [25].

Meanwhile, we obtained two different Cu(II) crystal complexes of GAA. One of them was a dimeric-copper(II)-bridge-carboxylate complex, tetrakis( $\mu$ -guanidinoacetic acid- $\kappa^2\text{O}:\text{O}'$ )bis[nitrate- $\kappa\text{O}$ -copper(II)],  $[\text{Cu}_2(\text{NO}_3)_2(\text{GAA})_4]$  [28]. This complex, in contrast with previous ones, presented an exclusive-oxygen coordination. The other complex, aqua[ $\mu$ -( $N^1$ -carboxylato-methylguanidino)oxidoacetato]( $\mu$ -guanidinoacetic acid)di-copper(II) nitrate dehydrate,  $[\text{Cu}_2(\text{C}_5\text{H}_6\text{N}_3\text{O}_5)(\text{C}_3\text{H}_7\text{N}_3\text{O}_2)\cdot\text{H}_2\text{O}]\text{NO}_3\cdot 2\text{H}_2\text{O}$ , presented a new ligand,  $\text{C}_5\text{H}_6\text{N}_3\text{O}_5$   $N,N'$ -guanidinodiacetic acid (Oag), a guanidine derivative, formed from GAA and copper(II) solution [29]. In this complex, GAA is again coordinated through both oxygen atoms of the bridged carboxylate group whereas the new ligand Oag was coordinated to two Cu(II) ions through three oxygen atoms and one nitrogen atom from the guanidino group. In order to understand the formation of we made an EPR study during different steps of the complex synthesis [30]. We proposed a mechanism of Oag formation based on a reaction between two  $\text{CuH}_2\text{GAA}$  precursor species, followed by a nucleophilic attack of the coordinated water to the  $\alpha$ -carbon of GAA, causing its desamidation as a consequence. The fragment resultant from the latter reaction then reacts with a non-coordinated GAA and forms Oag.

Following our studies on GAA, we have investigated its complexation behavior in the presence of Cu(II) and two amino acids, glycine (Gly) and serine (Ser) separately. With Gly, the aforementioned guanidino-carboxylate interactions with GAA should not be possible if Gly were coordinated through its carboxylate group. Ser besides presenting an interesting hydroxyl group in its structure, which may involve other interactions, is present in some enzymes, specifically serine endopeptidases, which are inhibited by guanidino groups [31]. Moreover, reduced serine phosphorylation of the creatine transporter is associated with increments in myocellular creatine content after starvation [32].

Herein, we report two novel Cu(II) complexes synthesized from GAA and a copper(II) solution in the presence of Gly or Ser. Each of such complexes presents a condensed amino acid residue formed by GAA and Gly or Ser with an elongation of the carbon chain. The X-ray structures of both complexes as well as their spectroscopic characterization are herein presented. In addition, we attempt to propose a mechanism for the formation of the new ligands, serine-3- $N$ -methylguanidino acetic acid and glycine-3- $N$ -methylguanidino acetic acid. Another interesting point for discussion, in addition to the elongation of the carbon chain, is the methylation on the N3 atom from GAA instead of on the  $\alpha$ -nitrogen. The synthesis of new guanidines has been intensively investigated since they play an important role in biological recognition sites and catalysis [33] and some of them are used in the design of drugs for different areas of application [34].

## 2. Experimental

### 2.1. Syntheses of the complexes *O,O',N,N'*-glycine-*N*-3-methylguanidinoacetic acid copper(II) [CuGly-mGAA] (**1**) and *O,O',N,N'*-serine-*N*-3-methylguanidinoacetic acid copper(II) [CuSer-mGAA] (**2**)

An aqueous solution of 3 mmol of guanidinoacetic acid (0.3513 g, Sigma-Aldrich) and 3 mmol of glycine (0.2252 g, Merck) or serine (0.3153 g, Merck) in 30 mL of deionized water was stirred at a temperature of 60 °C for 6 h until complete dissolution. A solution of 3 mmol (0.7248 g, Merck) of copper(II) nitrate in 5 mL of deionized water was then slowly added to the previous mixture, followed by stirring at a temperature of 60 °C for approximately 8 h. After that the mixture was cooled until 4 °C for 24 h. The mixture was filtered and the pH of the filtrate was adjusted to 4.3 with KOH 3 mol/L (Merck). After cooling the solution until 4 °C for 24 h, it was stocked in a glass vessel at room temperature. Slow evaporation of the solution resulted in blue needle crystals, which were washed with absolute ethanol (Merck) and dried at 50 °C for 2 h.

### 2.2. X-ray analyses

The crystal structures of the two complexes (CuGly-mGAA and CuSer-mGAA) were determined by X-ray diffraction. Data were collected in a Nonius KappaCCD diffractometer at  $T = 293$  K. The HKL DENZO and SCALEPACK programs [35] were used for cell refinement and data reduction.

### 2.3. Infrared spectroscopy

The infrared spectra were recorded on a Perkin–Elmer 2000 FT-IR spectrometer. Data were collected with a  $0.5\text{ cm}^{-1}$  interval with a resolution of  $4\text{ cm}^{-1}$ . The scanning speed was  $0.2\text{ cm s}^{-1}$  and 120 scans were performed. The samples were measured in the range of  $4000\text{--}370\text{ cm}^{-1}$  as KBr pellets, and in the range of  $710\text{--}30\text{ cm}^{-1}$  as polyethylene pellets.

### 2.4. DFT calculations

In order to correlate the structures obtained by X-ray diffraction with the IR spectra of the complexes we have chosen one of the complexes, complex **2**, to compare the experimental and calculated spectrum.

Vibrational assignments of the complex CuSer-mGAA (complex **2**) were carried out with the aid of density functional theory (DFT) calculations.

Ab initio optimization of the geometrical parameters, and hence structural analysis of the guanidoacetic–serinate Cu(II) complex, was carried out employing DFT levels [36–38] with B3LYP/6-31G and with B3LYP/6-311G basis sets, and the RHF/6-311G procedure.

## 3. Results and discussion

### 3.1. X-ray structure of the complexes

The equatorial coordination of copper atoms is similar for the two compounds herein described (Table 1). The ligands coordinate toward two oxygen atoms (O2 and O3) of different carboxylate groups and two nitrogen atoms (N1 and N4) to form the equatorial plane of the metal. Nitrogen N1 is positioned *trans* to oxygen O3. The equatorial planes of CuGly-mGAA and of CuSer-mGAA present almost planar *cis* configurations. Similar configurations were observed in other Cu(II) amino acids complexes,  $[\text{Cu}(\text{l-Arg})_2](\text{NO}_3)_2 \cdot 3\text{H}_2\text{O}$  [39],  $[\text{Cu}(\text{l-iso-leu})_2] \cdot \text{H}_2\text{O}$  [40] and  $[\text{Cu}(\text{Gly})_2] \cdot \text{H}_2\text{O}$  [41]. Bond angles in the equatorial plane of copper in CuSer-mGAA are similar to the values obtained for the Cu(II) amino acid complexes (Table 2). The O–Cu–N bond angles, inside each Cu-peptide ring, are acute (around 85°). Angles O–Cu–O and N–Cu–N, outside the Cu-peptide rings of these compounds, are obtuse. Compound Cu-Gly-mGAA, on the other hand, has all angles in the equatorial plane of copper close to 90°.

It is interesting to note the differences between N1 and N4: distances from least square planes (Table 3) show C2 and C3 closer to the least square plane towards Cu, O2, C1, N1 and O1 than C4 and C5 to the plane toward Cu, O3, C6, N4 and O4. As can be seen in Table 3, the deviation from the planes is stronger for CuSer-mGAA than for CuGly-mGAA. Atoms C2 and C3 of CuGly-mGAA are in the plane towards Cu, O2, C1, N1 and O1.

Copper axial coordination is different in the two compounds. One weak interaction between copper and the oxygen O4 ( $d[\text{Cu} \cdots \text{O4}] = 2.380(7)\text{ Å}$ ) of a second ligand (Fig. 2) is present in CuGly-mGAA. The structure of CuSer-mGAA (Fig. 3), on the other hand, has the axial neighborhood of the metal fulfilled by two copper–water interactions. One of these is weak, with  $d[\text{Cu} \cdots \text{O7}] = 2.500(4)\text{ Å}$ ; the other is very weak, with  $d[\text{Cu} \cdots \text{O6}] = 2.820(4)\text{ Å}$ . The ligands on the axial direction appear to affect the deviation of Cu from the least square planes towards its equatorial neighbor (Table 4), which is stronger in the axially less symmetric CuGly-mGAA ( $0.146(5)\text{ Å}$ ) than in the more symmetric CuSer-mGAA ( $0.084(2)\text{ Å}$ ).

The packing of Cu-Ser-mGAA (Fig. 3b) is formed by parallel layers of molecules. Molecules of neighbor layers are connected through hydrogen bonds involving the water molecules and the carboxylate oxygens (Tables 4 and 5).  $\text{N} \cdots \text{H} \cdots \text{O}$  hydrogen bonds also contribute to stabilize the crystal structure. The packing of Cu-Gly-mGAA (Fig. 2b), differently, is stabilized by the polymeric structure formed by molecules oriented perpendicularly to each other and linked through Cu–O4 bonds, as well as hydrogen bonds involving the water molecule and the carboxylate oxygens O4 and O1 of neighbor molecules.

Table 1  
Bond lengths (Å) and angles (°) for CuSer-mGAA and CuGly-mGAA

|                              | Cu-Ser-mGAA | Cu-Gly-mGAA |
|------------------------------|-------------|-------------|
| Bond lengths (Å)             |             |             |
| Cu(1)–O(2)                   | 1.937(3)    | 1.925(7)    |
| O(2)–C(1)                    | 1.287(6)    | 1.339(13)   |
| C(1)–O(1)                    | 1.240(5)    | 1.216(11)   |
| C(1)–C(2)                    | 1.510(7)    | 1.600(17)   |
| C(2)–N(1)                    | 1.450(6)    | 1.393(10)   |
| N(1)–Cu(1)                   | 1.930(4)    | 2.024(7)    |
| N(1)–C(3)                    | 1.299(6)    | 1.374(12)   |
| C(3)–N(2)                    | 1.341(6)    | 1.408(12)   |
| C(3)–N(3)                    | 1.366(6)    | 1.315(12)   |
| N(3)–C(4)                    | 1.424(6)    | 1.414(14)   |
| C(4)–N(4)                    | 1.493(6)    | 1.388(14)   |
| N(4)–Cu(1)                   | 1.986(4)    | 1.959(9)    |
| N(4)–C(5)                    | 1.479(7)    | 1.428(12)   |
| C(5)–C(6)                    | 1.536(9)    | 1.599(14)   |
| C(6)–O(3)                    | 1.281(6)    | 1.245(11)   |
| O(3)–Cu(1)                   | 1.960(3)    | 2.037(7)    |
| C(6)–O(4)                    | 1.235(6)    | 1.287(12)   |
| C(5)–C(7)                    | 1.527(7)    |             |
| C(7)–O(5)                    | 1.430(7)    |             |
| Cu(1)–O(7)                   | 2.500(3)    |             |
| Cu(1)–O(6)                   | 2.827(3)    |             |
| Cu(1)–O(4) <sup>1</sup>      |             | 2.382(7)    |
| Bond angles (°)              |             |             |
| N(1)–Cu(1)–O(2)              | 84.97(17)   | 89.0(4)     |
| N(1)–Cu(1)–O(3)              | 173.88(18)  | 165.6(3)    |
| O(2)–Cu(1)–O(3)              | 94.78(14)   | 88.6(3)     |
| N(1)–Cu(1)–N(4)              | 95.51(17)   | 91.4(3)     |
| O(2)–Cu(1)–N(4)              | 176.18(18)  | 177.6(5)    |
| O(3)–Cu(1)–N(4)              | 84.34(17)   | 90.4(3)     |
| C(1)–O(2)–Cu(1)              | 114.5(3)    | 110.9(8)    |
| C(6)–O(3)–Cu(1)              | 114.3(3)    | 109.5(7)    |
| C(3)–N(1)–C(2)               | 119.3(4)    | 120.4(9)    |
| C(3)–N(1)–Cu(1)              | 125.6(3)    | 130.1(7)    |
| C(2)–N(1)–Cu(1)              | 112.0(3)    | 109.4(6)    |
| C(3)–N(3)–C(4)               | 122.9(4)    | 117.4(9)    |
| C(5)–N(4)–C(4)               | 115.0(4)    | 127.8(10)   |
| C(5)–N(4)–Cu(1)              | 108.3(3)    | 104.9(6)    |
| C(4)–N(4)–Cu(1)              | 109.2(3)    | 113.4(8)    |
| O(1)–C(1)–O(2)               | 123.2(4)    | 118.1(12)   |
| O(1)–C(1)–C(2)               | 119.6(4)    | 123.6(11)   |
| O(2)–C(1)–C(2)               | 117.2(4)    | 118.3(10)   |
| N(1)–C(2)–C(1)               | 124.3(5)    | 125.4(11)   |
| N(1)–C(3)–N(2)               | 110.2(4)    | 112.4(9)    |
| N(1)–C(3)–N(3)               | 119.8(4)    | 121.3(9)    |
| N(2)–C(3)–N(3)               | 115.9(4)    | 113.2(9)    |
| N(3)–C(4)–N(4)               | 110.7(4)    | 132.4(11)   |
| N(4)–C(5)–C(6)               | 110.0(4)    | 117.5(8)    |
| O(4)–C(6)–O(3)               | 123.1(5)    | 117.4(10)   |
| O(3)–C(6)–C(5)               | 117.1(4)    | 117.2(10)   |
| O(4)–C(6)–C(5)               | 119.7(5)    | 125.3(9)    |
| O(5)–C(7)–C(5)               | 108.1(4)    |             |
| N(4)–C(5)–C(7)               | 110.6(5)    |             |
| C(7)–C(5)–C(6)               | 112.0(5)    |             |
| O(2)–Cu(1)–O(4) <sup>1</sup> |             | 97.2(3)     |
| N(4)–Cu(1)–O(4) <sup>1</sup> |             | 85.1(4)     |
| N(1)–Cu(1)–O(4) <sup>1</sup> |             | 103.2(3)    |
| O(3)–Cu(1)–O(4) <sup>1</sup> |             | 91.3(3)     |
| C(6)–O(4)–Cu(1) <sup>2</sup> |             | 130.8(7)    |

Symmetry operations: 1:  $X - 1/2, -Y - 1/2, -Z$ ; 2:  $X + 1/2, -Y - 1/2, -Z$ .

### 3.2. Infrared spectroscopy analyses

#### 3.2.1. Infrared spectroscopy analysis of CuGly-mGAA (complex 1)

The following discussion on infrared analysis has been based on comparisons with analogous complexes. The principal infrared data of complex **1** as well as of Gly [42], GAA [24], *trans*-Cu(Gly)<sub>2</sub> [42] and *cis*-Cu(GAA)<sub>2</sub> [24] are presented in Table 6.

Several bands can be observed in the 3500–3200 cm<sup>−1</sup> range. The first in 3536 cm<sup>−1</sup> is relative to the stretching modes of O–H of lattice water [42]. In addition, several other bands were observed in the same range, relative to stretching N–H modes of amines, in 3332 cm<sup>−1</sup>, 3422 cm<sup>−1</sup> and 3199 cm<sup>−1</sup>. The band in 1670 cm<sup>−1</sup> attributed to  $\nu$ C=N of the guanidino group from GAA was shifted to 1667 cm<sup>−1</sup> in *cis*-Cu(GAA)<sub>2</sub>, whereas it was not observed in complex **1**, probably indicating that this group has suffered significant modifications. This makes sense since complex **1** presents a methyl group bound to the terminal nitrogen from its guanidino group.

In the 1630–1380 cm<sup>−1</sup> range, the carboxylate asymmetric and symmetric stretching modes were observed probably coupled with amine deformation modes. Considering the number of carboxylate groups as well as the number of amines, the attempted assignments become very difficult.

Several new bands were observed in the 450–300 cm<sup>−1</sup> range. By comparing the same spectral region observed in *trans*-Cu(Gly)<sub>2</sub> and *cis*-Cu(GAA)<sub>2</sub>, the bands in 464 cm<sup>−1</sup> and 409 cm<sup>−1</sup> may be related approximately to  $\nu$ (Cu–N) coupled with other vibrational modes while those in 361 cm<sup>−1</sup> and 341 cm<sup>−1</sup> to  $\nu$ (Cu–O), also coupled with other framework vibrational modes. It has also been observed that the skeletal modes of GAA (436 cm<sup>−1</sup> and 319 cm<sup>−1</sup>) were absent, reflecting the modifications that occurred in its structure.

#### 3.2.2. Infrared spectroscopy analysis of CuSer-mGAA (complex 2)

Table 7 presents the principal infrared bands and their assignments of complex **2**, GAA [24], Ser [43] and *cis*-Cu(GAA)<sub>2</sub> [24].

The band in 3454 cm<sup>−1</sup> is relative to the stretching mode of O–H of lattice water. The other bands in the 3400–3200 cm<sup>−1</sup> range are probably relative to stretching N–H modes of amines. Analogously to complex **1**, the band in 1670 cm<sup>−1</sup> was not observed in **2**, for the same reasons mentioned above.

The bands in 1646 cm<sup>−1</sup>, 1558 cm<sup>−1</sup>, 1544 cm<sup>−1</sup>, 1466 cm<sup>−1</sup> and 1369 cm<sup>−1</sup> are assumed to correspond to asymmetric and symmetric stretching modes of the carboxylate group, probably coupled with amine deformation modes.

Several new bands were observed in the 450–300 cm<sup>−1</sup> range. The bands in 466 cm<sup>−1</sup> and 429 cm<sup>−1</sup> may be related to  $\nu$ (Cu–N), while those in 390 and 376 cm<sup>−1</sup> to  $\nu$ (Cu–O).



Table 2  
Geometrical parameters of the Cu coordination sphere (Å, °)

|          | CuGly-mGAA | CuSer-mGAA | [Cu(l-Arg) <sub>2</sub> ](NO <sub>3</sub> ) <sub>2</sub> · 3H <sub>2</sub> O | [Cu(l-isoleu) <sub>2</sub> ] · H <sub>2</sub> O | [Cu(gly) <sub>2</sub> ] · H <sub>2</sub> O |
|----------|------------|------------|--|---|--|
| Cu–O2    | 1.925(7)   | 1.937(3)   | 1.930(4)   | 1.948   | 1.957(9)                                   |
| Cu–O3    | 2.037(7)   | 1.960(3)   | 1.973(4)   | 1.953   | 1.946(9)                                   |
| Cu–N1    | 2.024(7)   | 1.930(4)   | 1.974(5)   | 1.989   | 1.984(10)                                  |
| Cu–N4    | 1.959(9)   | 1.986(4)   | 1.972(5)   | 1.995   | 2.021(11)                                  |
| O2–Cu–O3 | 88.6(3)    | 94.78(14)  | 94.3(2)  | 91.7  | 92.9(4)                                    |
| N1–Cu–N4 | 91.4(3)    | 95.51(17)  | 96.7(2)  | 98.6  | 96.6(4)                                    |
| O2–Cu–N1 | 89.0(4)    | 84.97(17)  | 84.5(2)  | 84.2  | 85.0(4)                                    |
| O3–Cu–N4 | 90.4(3)    | 84.34(17)  | 84.3(2)  | 84.5  | 85.4(4)                                    |

Table 3  
Distances (Å) of selected atoms to selected least square planes of CuGly-mGAA and CuSer-mGAA

| Plane      | Atom | Cu-Gly-mGAA | Cu-Ser-mGAA |
|------------|------|-------------|-------------|
| O2C1N1O1Cu | C2   | 0.008(12)   | 0.113(7)    |
|            | C3   | 0.057(16)   | 0.200(9)    |
| O3C6N4O4Cu | C4   | 0.669(22)   | 0.797(9)    |
|            | C5   | 0.100(14)   | 0.243(7)    |
| N1N4O3O2   | Cu   | 0.146(5)    | 0.084(2)    |

Similarly to complex **1**, the GAA bands in 436 cm<sup>−1</sup> and 319 cm<sup>−1</sup>, relative to skeletal modes, were absent in **2**.

### 3.3. Vibrational assignments

For the discussion of vibrational assignments, we will take the DFT values corrected by a scale factor of 0.9613 as a base of comparison with the 81 experimental wave numbers of the infrared spectra joined to second derivative bands. For an accurate description of the normal modes in the metal-ligand spectral range, as we have proposed in other works [44,45], we use the percentage of deviation of geometrical parameters (PDGP) from the equilibrium position. The PDGP can be also normalized to obtain

the percentage of participation of each internal vibrational coordinate that describes the framework vibrations.

#### 3.3.1. NH and CH stretching

We expected to observe a total of four bands pertaining to the asymmetric and symmetric N–H stretching normal modes. Within a large band centered on 3333 cm<sup>−1</sup>, we could identify absorption bands at 3676, 3568, 3452, 3340, 3299, 3263, 3242, 3140, 2922, 2896 and 2852 cm<sup>−1</sup>. These bands can be assigned according to DFT results to the vibrational modes  $\nu_{as}(\text{NH})$ ,  $\nu(\text{OH})$ ,  $\nu_s(\text{NH})$ ,  $\nu_s(\text{NH})$ ,  $\nu_s(\text{NH})$ ,  $\nu_s(\text{NH})$ ,  $\nu_{as}(\text{CH})$ ,  $\nu_{as}(\text{CH})$ ,  $\nu_{as}(\text{CH})$ ,  $\nu_{as}(\text{CH})$ ,  $\nu(\text{CH})$  methane,  $\nu_s(\text{CH})$  and  $\nu(\text{CH})$ , respectively. The second derivative spectrum shows bands at 3571, 3459, 3343, 3299, 3264, 242, 3129, 2961, 2898 and 2851 cm<sup>−1</sup>, presenting good correlation with the experimental ones. When we applied the Bellamy–Williams relationship [46] for primary amines  $\nu(a') = 345.5 + 0.876\nu(a'')$  to the experimental band found at 3676 cm<sup>−1</sup>, we obtained the value of 3565 cm<sup>−1</sup>, so we can conclude that the value calculated at 3695 cm<sup>−1</sup> by the DFT method could not be considered as the  $\nu(\text{OH})$  vibrational mode. The DFT calculated bands for these NH and CH stretching vibrational modes are in good agreement with experimental ones.

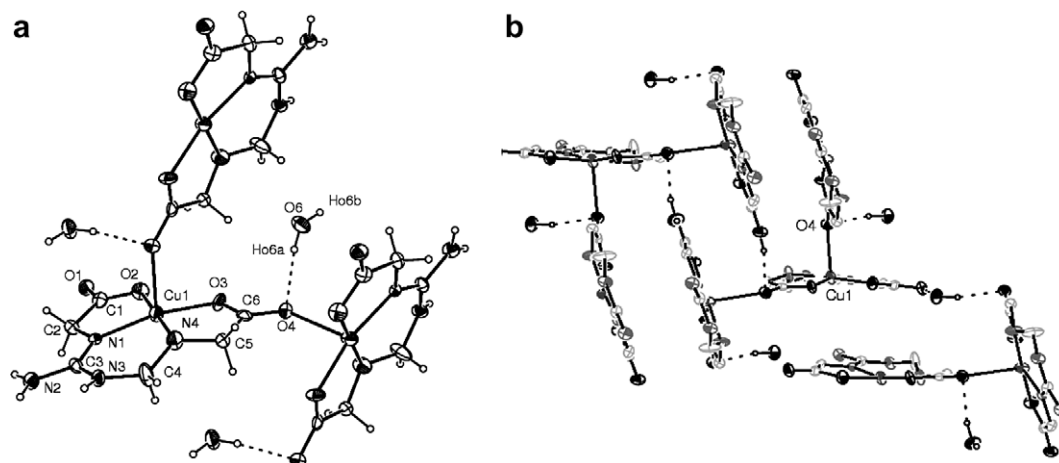


Fig. 2. ORTEP drawings of (a) the molecule of the monomer of CuGly-mGAA and its bonded neighbors, and (b) the packing of the crystal of CuGly-mGAA. Ellipsoids at 20% displacement level.

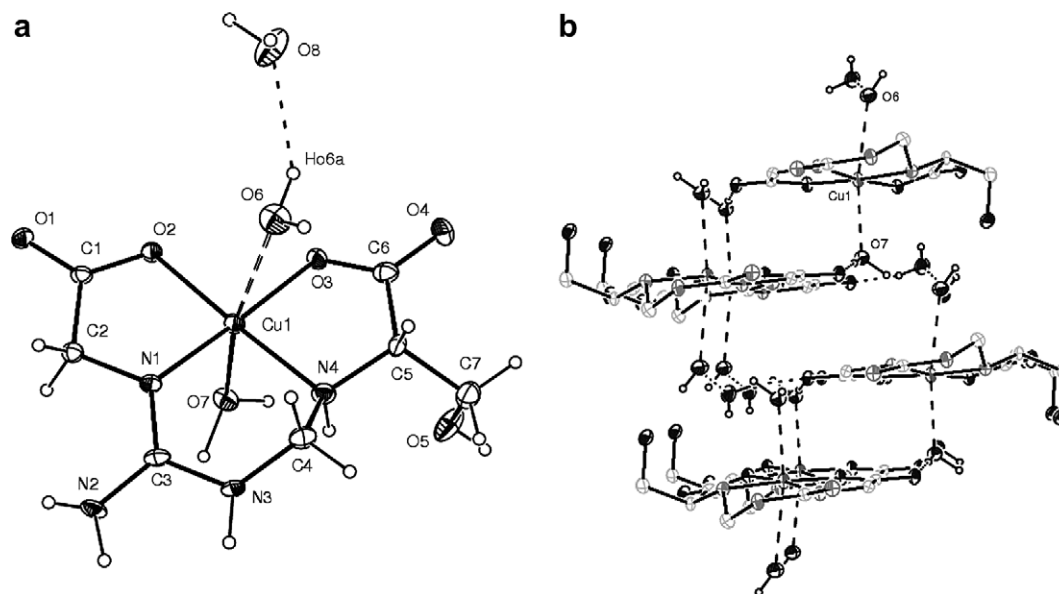


Fig. 3. ORTEP drawings of (a) the molecule of CuSer-mGAA with the water molecules that complete the asymmetric unit of the crystal, and (b) the packing of the crystal of CuSer-mGAA. Ellipsoids at 20% displacement level.

Table 4

Hydrogen bond parameters (Å, °) for CuSer-mGAA

| D–H...A                   | D–H (Å)  | H...A (Å) | D...A (Å) | D–H...A (°) |
|---------------------------|----------|-----------|-----------|-------------|
| <i>CuSer-mGAA</i>         |          |           |           |             |
| O6–HO6A...O8              | 0.869(4) | 2.063(4)  | 2.813(6)  | 144.1(3)    |
| N4–HN4...O7               | 0.91     | 2.74      | 3.152(6)  | 108.5       |
| O6–HO6B...O5 <sup>1</sup> | 0.861(4) | 1.943(4)  | 2.804(5)  | 178.1(3)    |
| O7–HO7A...O6 <sup>2</sup> | 0.986(3) | 1.865(4)  | 2.813(5)  | 160.5(2)    |
| O7–HO7B...O1 <sup>3</sup> | 1.104(3) | 1.646(3)  | 2.747(4)  | 175.0(2)    |
| N2–HN2B...O7 <sup>3</sup> | 0.86     | 2.12      | 2.918(5)  | 153.6       |
| O8–HO8A...O1 <sup>4</sup> | 0.977(4) | 1.797(3)  | 2.756(5)  | 166.1(3)    |
| O5–HO5...O4 <sup>5</sup>  | 0.82     | 1.91      | 2.707(5)  | 164.4       |
| N2–HN2A...O2 <sup>6</sup> | 0.86     | 2.02      | 2.805(6)  | 150.9       |
| N3–HN3...O3 <sup>7</sup>  | 0.86     | 2.24      | 3.084(5)  | 166.6       |

Symmetry operations: 1:  $X - 1, Y, Z$ ; 2:  $X + 1, Y, Z$ ; 3:  $-X + 2, Y - 0.5, -Z + 1$ ; 4:  $-X + 1, Y + 0.5, -Z + 1$ ; 5:  $-X + 3, Y - 0.5, -Z + 2$ ; 6:  $X, Y - 1, Z$ ; 7:  $X, Y - 1, Z$ .

Table 5

Hydrogen bond parameters (Å, °) for CuGly-mGAA

| D–H...A                   | D–H (Å)  | H...A (Å) | D...A (Å) | D–H...A (°) |
|---------------------------|----------|-----------|-----------|-------------|
| <i>Cu-Gly-mGAA</i>        |          |           |           |             |
| O6–HO6A...O4              | 0.860(7) | 1.969(7)  | 2.818(10) | 168.8(6)    |
| O6–HO6B...O1 <sup>1</sup> | 0.869(6) | 2.075(7)  | 2.940(9)  | 173.5(5)    |
| N2–HN2A...O6 <sup>2</sup> | 0.86     | 2.03      | 2.816(11) | 151.6       |
| N3–HN3...O3 <sup>3</sup>  | 0.86     | 2.49      | 3.283(12) | 152.7       |
| N3–HN3...O4 <sup>3</sup>  | 0.86     | 2.56      | 3.288(12) | 143.2       |
| N4–HN4...O1 <sup>4</sup>  | 0.91     | 2.33      | 3.073(13) | 138.8       |

Symmetry operations: 1:  $-X + 1.5, -Y - 1, Z - 0.5$ ; 2:  $-X + 1.5, -Y, Z + 0.5$ ; 3:  $X, Y + 1, Z$ ; 4:  $-X + 1.5$ .

### 3.3.2. C=O stretching

Observing the geometrical structure of the guanidoacetate-serinate Cu(II) complex depicted in Fig. 4, we can infer only one asymmetrical and one symmetrical C=O stretch-

ing. As it is well known, the band absorption of carbonyl groups is located in the region of  $\sim 1700\text{--}1500\text{ cm}^{-1}$ , commonly in a higher energy region than the absorption bands pertaining to the HNH bending vibrational modes. In the infrared spectrum, we can observe two bands at  $1650\text{ cm}^{-1}$  and at  $1623\text{ cm}^{-1}$ . The second derivative of the spectrum and the band deconvolution analysis include values at  $1650\text{ cm}^{-1}$  and at  $1623\text{ cm}^{-1}$ , respectively. By means of the DFT procedure with B3LYP/6-311G and 6-311G basis sets we can assign the experimental band found at  $1650\text{ cm}^{-1}$  (IR, second derivative) to the  $\nu_s(\text{C=O})$  vibrational mode, and the band found at  $1623\text{ cm}^{-1}$  to the  $\nu_{as}(\text{C=O})$  vibrational mode. The match between calculated and experimental values for the  $\nu(\text{C=O})$  stretching was excellent.

### 3.3.3. HNH and HCH bending

In the infrared spectrum we can observe four bands at 1721, 1500 (1511 second derivative), 1470 (second derivative), 1466, 1423 (1428 second derivative), 1390, 1320 (1322 second derivative), 1283 (second derivative) 1279 and 1256 (second derivative), which can be correlated with the scaled DFT:B3LYP/6-311G values: 1642, 1518, 1487, 1483, 1427, 1388, 1317, 1295, 1283 and  $1248\text{ cm}^{-1}$ . These bands can be assigned principally to  $\delta(\text{HNH})\text{wagg}$ ,  $\delta(\text{HCH})\text{wagg}$ ,  $\delta(\text{HCH})\text{wagg}$ ,  $\delta(\text{HCH})\text{wagg}$ ,  $\delta(\text{HCH})\text{wagg}$ ,  $\delta(\text{HCH})\text{twist}$ ,  $\delta(\text{HCH})\text{twist}$ ,  $\delta(\text{HCH})\text{twist}$  and  $\delta(\text{HCH})\text{twist}$ , respectively. Rocking vibrations according to the DFT calculations can be assigned as follows:  $1103\text{ cm}^{-1}$  to  $\rho(\text{CH})_2 + \rho(\text{NH}_2)$ ,  $1071\text{ cm}^{-1}$  to  $\rho(\text{OH}) + \rho(\text{NH}_2)$ ,  $1043\text{ cm}^{-1}$  to  $\rho(\text{CH})_2 + \delta(\text{HNH})\text{twist}$ .

### 3.3.4. CN, CO, and CC stretching vibrations

A natural and considerable mixture of the internal coordinates describing isolated C–N, C–O, C–C stretching is

Table 6

Principal infrared bands (in  $\text{cm}^{-1}$ ) of CuGly-mGAA (complex 1), Gly, GAA, *trans*-Cu(Gly)<sub>2</sub> and *cis*-Cu(GAA)<sub>2</sub>

| Complex 1                                      | GAA <sup>a</sup> | Gly <sup>b</sup> | <i>trans</i> -Cu(Gly) <sub>2</sub> <sup>a</sup> | <i>cis</i> -Cu(GAA) <sub>2</sub> <sup>b</sup> | Approximate assignments                  |
|--|------------------|------------------|---|---|--|
| 3535   |                  |                  |   |   | $\nu(\text{O-H})$ (water)                |
| 3422, 3332, 3199                               | 3385, 3303, 3173 |                  | 3320, 3260                                      | 3336, 3229                                    | $\nu(\text{N-H})$                        |
| 2930, 2890                                     |                  |                  |   |   | $\nu(\text{C-H})$                        |
| 2367, 2344                                     |                  |                  |   |   | combination bands                        |
|  | 1670             |                  |   | 1669  | $\nu(\text{C=N})$ (guanidino)            |
| 1638, 1606, 1585, 1561, 1541, 1533, 1397, 1385 |                  |                  |   | 1636  | $\nu(\text{C=O}) + \delta(\text{H-N-H})$ |
|  | 1626             |                  | 1608  | 1611  | $\delta(\text{H-N-H})$                   |
|  | 1582             |                  | 1593  | 1566  | $\nu_{\text{as}}(\text{COO}^-)$          |
|  | 1411             |                  | 1392  | 1405  | $\nu_{\text{s}}(\text{COO}^-)$           |
| 464, 409                                       |                  |                  | 481   | 446, 410                                      | $\nu(\text{Cu-N})$ coupled               |
| 361, 341                                       |                  |                  | 333   | 351, 328                                      | $\nu(\text{Cu-O})$ coupled               |
|  | 436              |                  |   | 436   | skeletal mode                            |
|  | 319              |                  |   | 319   | skeletal mode                            |

<sup>a</sup> Ref. [24].<sup>b</sup> Ref. [40].

Table 7

Principal infrared bands (in  $\text{cm}^{-1}$ ) of CuSer-mGAA (complex 2), GAA, Ser, and *cis*-Cu(GAA)<sub>2</sub>

| Complex 2              | GAA <sup>a</sup> | Ser <sup>b</sup>  | <i>cis</i> -Cu(GAA) <sub>2</sub> <sup>a</sup> | Attempted assignments                     |
|------------------------|------------------|---|---|---|
| 3676, 3568, 3542, 3340 | 3385, 3303, 3173 | 3610, 3556, 3540  |   | $\nu(\text{O-H})$                         |
| 2922, 2896             |                  | 3426, 3344, 3349(R) <sup>c</sup> , 3276(R) <sup>c</sup> | 3336, 3229                                    | $\nu(\text{N-H})$                         |
| 2362, 2342, 2332       |                  | 2966(R) <sup>c</sup> , 2903(R) <sup>c</sup>             |   | $\nu(\text{C-H})$                         |
| 1650, 1622             |                  |   |   | combination bands                         |
| 1682                   | 1670             |   | 1669  | $\nu(\text{C=O})$                         |
|                        |                  | 1618(R) <sup>c</sup> , 1592(R) <sup>c</sup>             | 1636  | $\nu(\text{C=N})$ (guanidino)             |
| 1721, 1423             | 1626             | 1646, 1624, 1608  | 1611  | $\nu(\text{COO}^-) + \delta(\text{NH}_2)$ |
|                        | 1582             |   | 1566  | $\delta(\text{NH}_2)$                     |
|                        | 1411             |   | 1405  | $\nu_{\text{as}}(\text{COO}^-)$           |
|                        |                  | 1374, 1349(R) <sup>c</sup>                              |   | $\nu_{\text{s}}(\text{COO}^-)$            |
| 596, 377, 317, 247     |                  |   | 446, 410                                      | $\delta(\text{OH}) + \nu(\text{C-O})$     |
| 340,247                |                  |   | 351, 328                                      | $\nu(\text{Cu-N})$ coupled mode           |
|                        | 436              |   | 436   | $\nu(\text{Cu-O})$ coupled mode           |
|                        | 319              |   | 319   | skeletal mode                             |

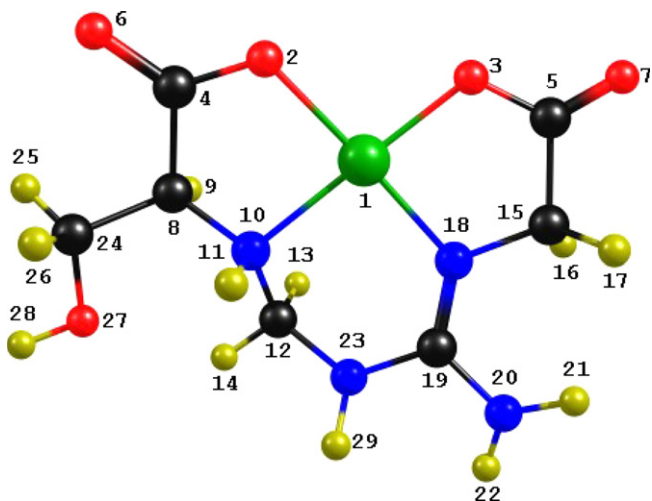
<sup>a</sup> Ref. [24].<sup>b</sup> Ref. [31].<sup>c</sup> Ref. [58].

Fig. 4. Calculated DFT:B3LYP/6-311G geometrical structure of CuSer-mGAA.

found in the normal modes and is physically meaningful. For the guanidoacetic-serinate Cu(II) complex, the following infrared coupled bands can be assigned principally as 1227 ( $\text{IR}$ )  $\text{cm}^{-1}$  to  $\nu_{\text{s}}(\text{CO})$ ; 1143  $\text{cm}^{-1}$  to  $\nu_{\text{s}}(\text{CN})$ ; 1008  $\text{cm}^{-1}$  to  $\nu_{\text{s}}(\text{CN})$ ; 993  $\text{cm}^{-1}$  to  $\nu_{\text{s}}(\text{CN})$ ; 956 to  $\nu(\text{CO})$  and 878  $\text{cm}^{-1}$  to  $\nu(\text{CC})$ .

### 3.3.5. Skeletal framework vibrations

As we have pointed out in other publications [44,45,47,48], a clear identification of the metal–ligand vibrations is not straightforward due to the higher mixture of different internal coordinates that take part in the description of the normal mode. In order to analyze the normal modes below 600  $\text{cm}^{-1}$  we will describe the most accurate assignment we were able to deduce through the study of the distorted geometries of the normal modes described by the ab initio DFT:B3LYP/6-311G procedures. Our goal was to identify which bond lengths and

bond angle bending parameters had greater participation in the description of the normal mode.

Fig. 4 displays the distorted geometry of the normal modes for the metal–ligand vibrations obtained through the free CHEMKRAFT program [49].

### 3.4. Proposal of a mechanism for the formation of Gly-mGAA and Ser-mGAA

Due to the interesting formation of new amino acid derivatives, a preliminary mechanism for their synthesis is proposed here (Fig. 5). We have based this proposal on previous work on the desamidation of copper(II) complexes of GAA analyzed by epr [30] as well as on data on guanidination reactions involving amino acids, phosphates and collagen [50–57] and also on methyltransferases. Some of guanidination [50] and methyltransferases [53] reactions are mediated by zinc(II) ions or zinc(II) coordination in a similar way that we propose here for Cu(II).

Nevertheless, we omitted copper(II) complexes from this mechanism because we were not able to analyze intermediate species. However, we do know that Cu(II) or its complexes may act both as a catalysts or template sites.

The proposed mechanism comprises two steps, both of them involving nucleophilic attack. It is interesting to note the similarity with the catalytic mechanism proposed for arginine deimination, with the difference of which carbon atom is attacked: the amidino one in the case of arginine

deimination and the  $\alpha$ -carbon in our proposed mechanism [58].

Step one is based on a deguanidination reaction between two GAA species in the presence of Cu(II). Guanidination reactions are used in reactions of biological relevance such as the synthesis of L-canavanine [50], the modification of a toxic enzyme from snake venom [51], the synthesis of thrombin inhibitor [52] and also the guanidination of the phosphate linkage towards cationic phosphoramidate oligonucleotides [55]. Deguanidination modified monomeric collagen in such a way that it prevented it from polymerization and to inducing platelet aggregation [54].

In step one, the terminal amino group from GAA makes a nucleophilic attack at  $\alpha$ -carbon from another GAA, followed by a deguanidination reaction, generating intermediate I: guanidino-*N,N'*-diacetic acid and guanidine (a good leaving group). A rather similar process has already been proposed between two GAA copper(II) complexes [30] by our group. Cu(II) is probably involved in the coordination through the oxygen atoms from the carboxylate group, similarly to what happens in the desamidation process [30], which favors the nucleophilic attack on the  $\alpha$ -carbon. The proposed intermediate I, guanidino-2,4-*N,N'*-diacetic acid, is essential to the elongation of the carbon chain.

In step two the  $\alpha$ -amino group from glycine or serine makes a nucleophilic attack at C-2 from intermediate I, followed by a decarboxylation process. The copper coordination is also assumed to mediate this nucleophilic attack and a Cu(II)/Cu(I) redox system may help on the decarboxylation reaction in addition to the heating experimental conditions.

As a final result, glycine-2-*N*-methyl guanidinoacetic acid or serine-2-*N*-methyl-guanidino acetic acid are formed and both of them act as a quadridentate ligand, using the oxygen atoms from the carboxylate groups and two nitrogen atoms (Fig. 4).

## 4. Conclusions

Two novel Cu(II) complexes were synthesized involving new condensed synthetic amino acids: one is glycine-3-*N*-methylguanidino acetic acid (Gly-mGAA), which results from the reaction between GAA and glycine, with an increase of one carbon in the chain; and the second is a similar ligand that is the product of the reaction between GAA and serine, that is, serine-3-*N*-methylguanidino acetic acid (Ser-mGAA). It is important to remark that this elongation of the carbon chain in both cases was performed in aqueous solution in the presence of Cu(II).

This can represent important mechanisms both for the synthesis of new guanidines derivatives and for methylation or peptide formation with biological molecules. Modifications in the precursor of GAA, arginine, for example, can be related to changes in the immunogenicity of proteins and peptides and can create self-antigens that induce autoimmune responses [57]. If these serine or glycine GAA adducts are catalyzed by enzymes in our organisms

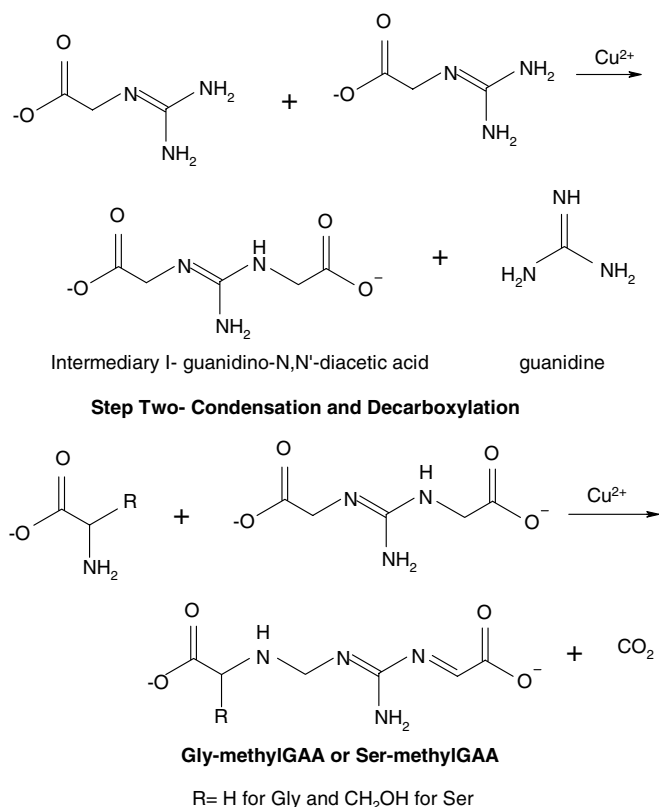


Fig. 5. Proposed mechanism for Gly-mGAA and Ser-mGAA.



through an alternative biological pathway, creatine biosynthesis will be impaired, resulting in a dysfunction similar to guanidinomethyltransferase deficiency.

Deguanidination reactions instead of desamidation should also prevent GAA biosynthesis, formed by the desamidation of arginine.

In addition, an important contribution on how GAA can react with other amino acids was proposed as well as how elongation of their carbon chain can be made in aqueous solution in the presence of Cu(II).

## Acknowledgements

The authors thank FAPESP (B.L.R.), CAPES (O.V.) and CNPq (J.M.R., J.F., C.A.T.S.).

## Appendix A. Supplementary material

CCDC 256924 and 256925 contain the supplementary crystallographic data for this paper. These data can be obtained free of charge via <http://www.ccdc.cam.ac.uk/conts/retrieving.html>, or from the Cambridge Crystallographic Data Centre, 12 Union Road, Cambridge CB2 1EZ, UK; fax: (+44) 1223-336-033; or e-mail: [deposit@ccdc.cam.ac.uk](mailto:deposit@ccdc.cam.ac.uk). Supplementary data associated with this article can be found, in the online version, at [doi:10.1016/j.poly.2007.05.029](https://doi.org/10.1016/j.poly.2007.05.029).

## References

- [1] M. Takeda, S. Nakayama, Y. Tomino, Y. Jung, H. Endou, H. Koide, in: P. P. Deyn, B. Marescau, V. Stalon, I.A. Qureshi (Eds.), *Guanidino Compounds in Biology and Medicine*, John Libbey & Company Ltd., 1992, pp. 153–157.
- [2] S. Stöckler, U. Holzbach, F. Hanefeld, I. Marquardt, G. Helms, M. Reuquart, W. Hanicke, J. Frahm, *Pediatr. Res.* 36 (1994) 409.
- [3] A. Neu, H. Neuheoff, G. Trube, S. Fehr, K. Ulrich, J. Roeper, D. Isbrandt, *Neurobiol. Dis.* 11 (2002) 298.
- [4] A.I. Zugno, F.M. Stefanello, E.L. Streck, T. Calcagnotto, C.M.D. Wannmacher, M. Wajner, A.T.S. Wyse, *Int. J. Develop. Neurosci.* 21 (2003) 183.
- [5] M.G. Alessandri, L. Celati, R. Battini, F. Baldinotti, C. Item, V. Leuzzi, G. Cioni, *Anal. Biochem.* 331 (2004) 189.
- [6] A. Shulze, F. Ebinger, D. Rating, E. Mayaetepek, *Mol. Genet. Metab.* 74 (2001) 413.
- [7] V. Leuzzi, M.C. Bianchi, M. Tosetti, C. Carducci, C.A. Cerquiglioni, G. Cioni, I. Antonozzi, *Neurology* 55 (2000) 1407.
- [8] A. Schulze, T. Hess, R. Wevers, E. Mayatepek, P. Bachert, B. Marescau, M.V. Knopp, P.P. Deyn, H.J. Bremer, D. Rating, *J. Pediatr.* 131 (1997) 626.
- [9] S. Stöckler, U. Holzbach, F. Hanefeld, I. Marquardt, G. Helms, M. Reuquart, et al., *Pediatr. Res.* 36 (3) (1994) 409.
- [10] S. Stöckler, B. Marescau, P.P. De Deyn, J. Trijbels, F. Hanefeld, *Metabolism* 46 (10) (1997) 1189.
- [11] A. Shulze, *Mol. Cell Biochem.* 244 (1–2) (2003) 143.
- [12] M. Ishizaki, H. Kitamura, Y. Taguma, K. Aoyagi, M. Narita, in: P. Deyn, B. Marescau, V. Stalon, I.A. Qureshi (Eds.), *Guanidino Compounds in Biology and Medicine*, John Libbey & Company Ltd., 1992, pp. 275–280.
- [13] B.D. Cohen, H. Patel, in: P.P. Deyn, B. Marescau, V. Stalon, I.A. Qureshi (Eds.), *Guanidino Compounds in Biology and Medicine*, John Libbey & Company Ltd., 1992, pp. 255–260.
- [14] O. Levillain, B. Marescau, P.P. Deyn, in: P.P. Deyn, B. Marescau, I.A. Qureshi, A. Mori (Eds.), *Guanidino Compounds in Biology and Medicine*, vol. 2, John Libbey & Company Ltd., 1997, pp. 289–297.
- [15] A. Neu, H. Neuheoff, G. Trube, K. Ulrich, J. Roeper, D. Isbrandt, *Neurobiol. Dis.* 11 (2) (2002) 298.
- [16] A.I. Zugno, F.M. Stefanello, E.L. Streck, T. Calcagnotto, C.M.D. Wannmacher, M. Wajner, A.T.S. Wyse, *Int. J. Develop. Neurosci.* 21 (2003) 183.
- [17] K. Sugiyama, A. Ohishi, H. Syiu, H. Takeuchi, *J. Nutr. Sci. Vitaminol.* 35 (1989) 613.
- [18] J. Verhelst, J. Berwaerts, B. Marescau, R. Abs, H. Neels, C. Mahler, *Metab. Clin. Exp.* 46 (1997) 1063.
- [19] A. Mori, M. Kohno, T. Masumizu, Y. Noda, L. Packer, *Biochem. Mol. Biol. Int.* 40 (1996) 135.
- [20] P.P. Deyn, B. Marescau, R. D'Hooge, I. Possemiers, J. Nagler, C.H. Mahler, *Neurochem. Int.* 27 (1995) 227.
- [21] M. Kuroda, *Nephron* 65 (1993) 605.
- [22] M. Yasuda, K. Sugahara, J. Zhang, T. Shuin, H. Kodama, *Physiol. Chem. Phys. Med NMR* 32 (2000) 119.
- [23] J. Felcman, J.L. Miranda, J. Braz, *Chem. Soc.* 8 (6) (1997) 575.
- [24] J.L. Miranda, J. Felcman, *Synth. React. Inorg. Met-Org Chem.* 31 (5) (2001) 873.
- [25] J.L. Miranda, J. Felcman, *Polyhedron* 22 (2003) 225.
- [26] J.A. Tainer, E.D. Getzoff, J.S. Richard, D.C. Richardson, *Nature* 306 (1983) 284.
- [27] R. Wyatt, J. Sodoroski, *Science* 280 (1998) 284.
- [28] J.L. Miranda, J. Felcman, J.L. Wardell, J.S. Skakle, *Acta Crystallogr., Sect. C* 58 (2002) m471.
- [29] J. Felcman, R. Alan Howie, J.L. Miranda, J.M.S. Skakle, J.L. Wardell, *Acta Crystallogr., Sect. C* 59 (2003) m103.
- [30] J.L. Miranda, J. Felcman, O. Versiane, M.H. Herbst, *Inorg. Chem. Commun.* 7 (2004) 1198.
- [31] Y. Yamauchi, T. Sugimoto, K. Sueyoshi, Y. Oji, K. Tanaka, *Phytochemistry* 58 (5) (2001) 677.
- [32] C.R. Zhao, L. Shang, W. Wang, D.O. Jacobs, *J. Surg. Res.* 105 (1) (2002) 10.
- [33] C.L. Hannon, E.V. Auslyn, in: H. Dugas, F.P. Schmidtchen (Eds.), *Bioorganic Chemistry Frontiers*, vol. 3, Springer, Berlin, 1993, p. 192.
- [34] J.L. Grenhil, P. Lue, in: G.P. Ellis, D.K. Luscombe (Eds.), *Progress in Medicinal Chemistry*, vol. 30, Elsevier Science, New York, 1993 (Chapter 5).
- [35] Enraf-Nonius COLLECT. Nonius BV, Delft, The Netherlands (1997–2000).
- [36] R.G. Parr, W. Yang, *Density-Functional Theory of Atoms and Molecules*, Oxford University Press, Oxford, 1989.
- [37] A.D. Becke, *J. Chem. Phys.* 98 (1993) 1372.
- [38] M.J. Frisch, G.W. Trucks, H.B. Schlegel, G.E. Scuseria, M.A. Robb, J.R. Cheeseman, V.G. Zakrzewski Jr., J.A. Montgomery, R.E. Stratmann, J.C. Burant, S. Dapprich, J.M. Millam, A.D. Daniels, K.N. Kudin, M.C. Strain, O. Farkas, J. Tomasi, V. Barone, N.M. Cossi, R. Cammi, B. Mennucci, C. Pomelli, C. Adamo, S. Clifford, J. Ochterski, G.A. Peterson, P.Y. Ayala, Q. Cui, K. Morokuma, D.K. Malick, A.D. Rabuck, K. Raghavachari, J.B. Foresman, J. Cioslowski, J.V. Ortiz, A.G. Baboul, B.B. Stepanov, G. Liu, A. Liashenko, P. Piskorz, I. Komaromi, R. Gomperts, R.L. Martin, D.J. Fox, T. Keith, M.A. Al-Laham, C.Y. Peng, A. Nanayakkara, C. González, M. Challacombe, P.M.W. Gill, B. Johnson, W. Chen, M.W. Wong, J.L. Andresw, C. González, M. Head-Gordon, E.S. Repogle, J.A. Pople, *GAUSSIAN 98*, Revision A.7, Gaussian Inc., Pittsburgh, PA, 1998.
- [39] H. Masuda, A. Odani, T. Yamazaki, T. Yajima, O. Yamauchi, *Inorg. Chem.* 32 (1993) 1111.
- [40] C.M. Weeks, A. Cooper, D.A. Norton, *Acta Crystallogr., Sect. B* 25 (1969) 443.
- [41] H.C. Freeman, M.R. Snow, I. Nitta, K. Tomita, *Acta Cryst.* 17 (1964) 1463.
- [42] K. Nakamoto, *Infrared and Raman Spectra of Inorganic and Coordination Compounds – Part B: Applications in Coordination*,

- Organometallic, and Bioinorganic Chemistry, 5th ed., Wiley, 1997, pp. 53, 63, 65.
- [43] B. Lambie, R. Ramaekers, G. Maes, J. Phys. Chem. 108 (2004) 10426.
- [44] C.A. Téllez S, E. Hollauer, M.A. Mondragón, V.M. Castaño, Spectrochim. Acta A 60 (2004) 2171.
- [45] C.A. Téllez, E. Hollauer, M.A. Mondragón, V.M. Castaño, Spectrochim. Acta A 57 (2001) 993.
- [46] L.J. Bellamy, R.L. Williams, Spectrochim Acta 9 (1957) 341.
- [47] J.M. Ramos, O. Versiane, J. Felcman, C.A. Téllez S, FT-IR vibrational spectrum and DFT: B3LYP/6-311G structure and vibrational analysis of bis-serinenickel (ii) complex: [Ni (Ser)<sub>2</sub>], Spectrochim. Acta A 67 (3–4) (2007) 1046.
- [48] J.M. Ramos, O. Versiane, J. Felcman, C.A. Téllez S, FT-IR vibrational spectrum and DFT: B3LYP/6-31G structure and vibrational analysis of guanidinoaceticserinenickel (II) complex: [Ni(GAA)(Ser)], Spectrochim. Acta A 67 (3–4) (2007) 1037.
- [49] CHEMCRAFT Software <<http://www.chemkraftprog.com/order.html>>.
- [50] A.J. Ozinskas, G.A. Rosenthal, Bioorg. Chem. 14 (2) (1986) 157.
- [51] A.S. Babu, T.V. Gowda, Toxicon 32 (6) (1994) 749.
- [52] J. Deng, Y. Hamada, T. Shioiri, Tetrahedron Lett. 37 (13) (1996) 2261.
- [53] M. Machuqueiro, T. Darbre, J. Inorg. Biochem. 94 (2003) 193.
- [54] Chung-Lieh Wang, T. Miyata, B. Weksler, A.L. Rubin, K.H. Stenzel, Biochim. Biophys. Acta 544 (3) (1978) 555.
- [55] T. Michel, F. Debart, J.-J. Vasseur, Tetrahedron Lett. 44 (35) (2003) 6579.
- [56] G.A. Rosenthal, L. Harper, Insect Biochem. Mol. Biol. 26 (4) (1996) 389.
- [57] M.A.M. van Boekel, W.J. Van Venrooij, Autoimmun. Rev. 2 (2003) 57.
- [58] Y. Huang, J. Komoto, K. Konishi, Y. Takata, H. Ogawa, T. Gomi, M. Fujioka, J. Mol. Biol. 298 (2000) 149.